Monte Carlo shell model and its application to exotic nuclei

Yutaka Utsuno
Japan Atomic Energy Agency

Collaborators
T. Otsuka (Tokyo), T. Mizusaki (Senshu), M. Honma (Aizu), N. Shimizu (Tokyo)

Contents

- Brief introduction of the Monte Carlo shell model
- Structure of exotic nuclei around N=20
- Recent understanding of the shell evolution

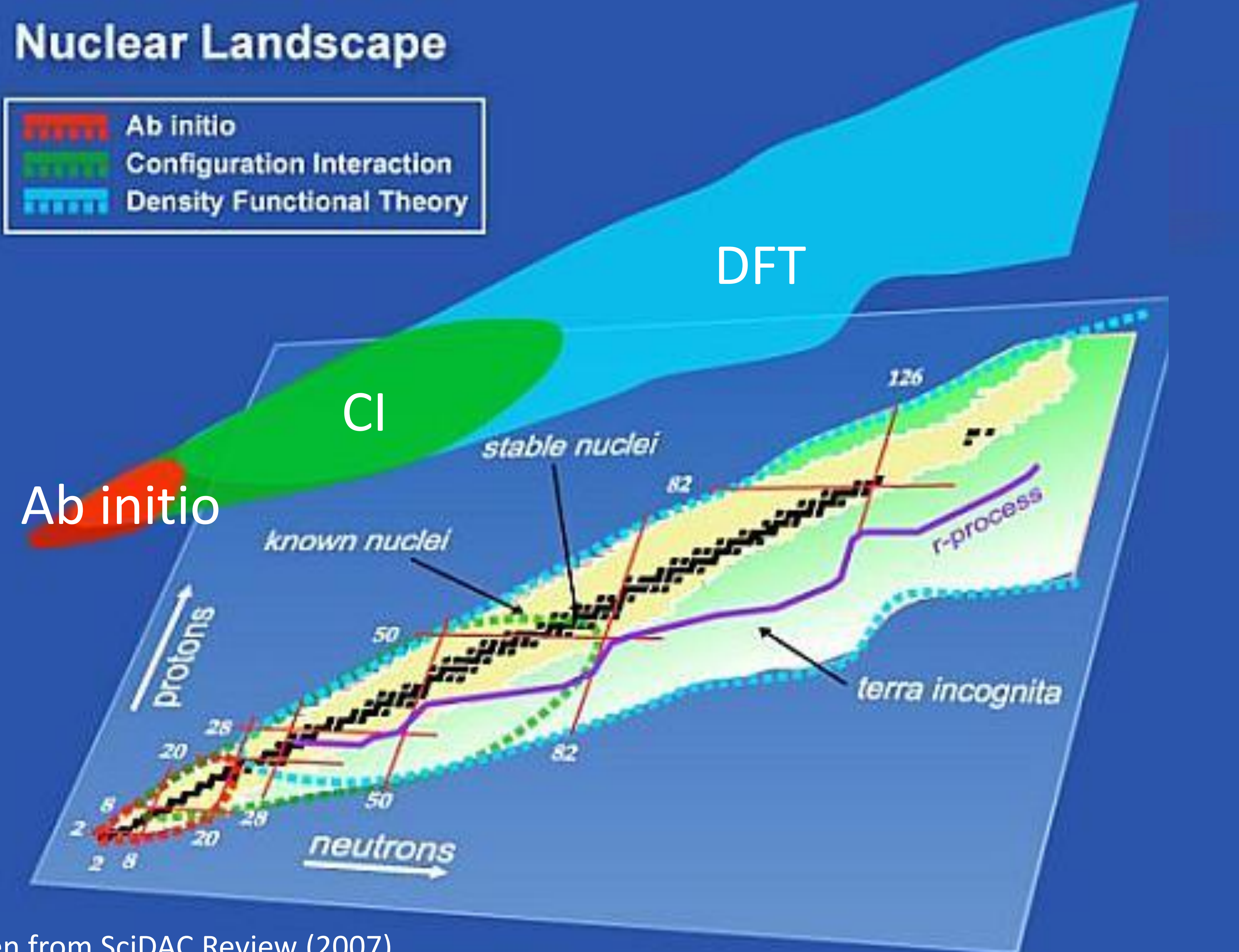

Taken from SciDAC Review (2007)

Even with-core shell model …

- Exponential wall

$$D=\binom{N_{sp}(\pi)}{N_p(\pi)}\times\binom{N_{sp}(\nu)}{N_p(\nu)}$$

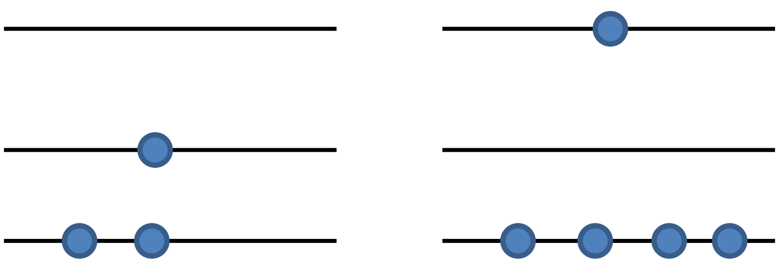

Shell model dimension for N=Z pf-g shell nuclei (without symmetry consideration)

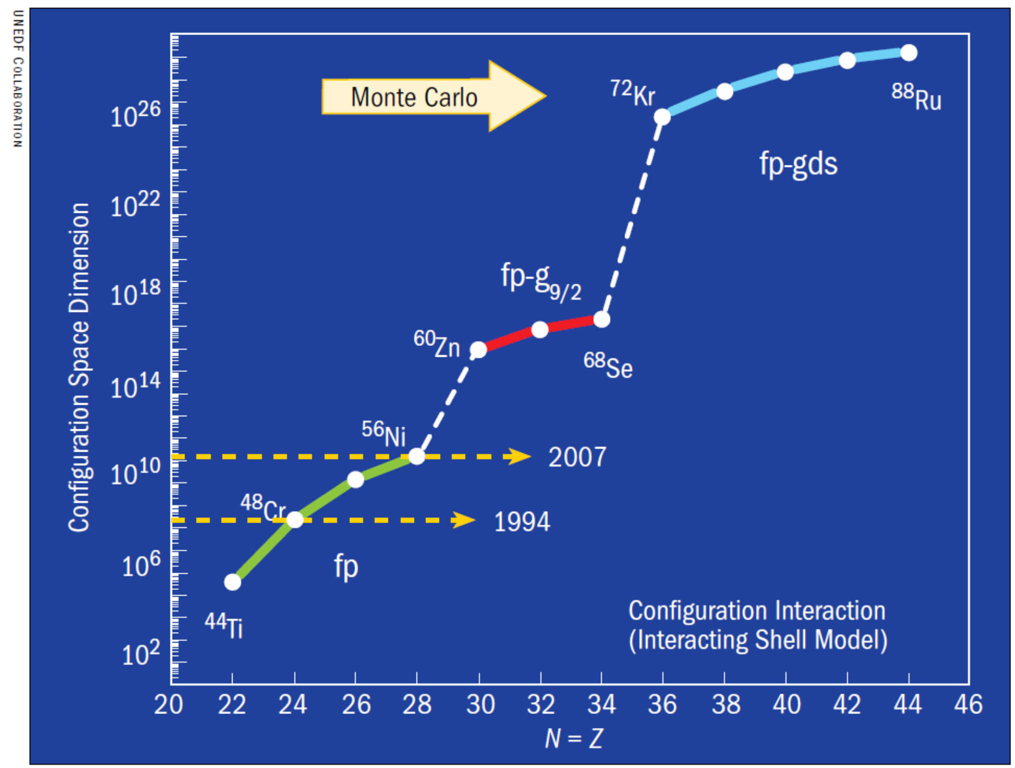

Taken from SciDAC Review (2007)

Current situation

- Light nuclei (p shell and sd shell in near future)
  - Ab initio shell model approach
  - Bare NN force can be used such as JISP16.
- Heavier nuclei (up to ^{132}Sn region)
  - Conventional shell model
  - Effective interaction
- What is needed
  1. A tool to make large-scale nuclear calculation possible
     - Monte Carlo shell model (MCSM)
  2. Good interaction
     - New findings about the evolution of the shell structure

Brief introduction of the Monte Carlo shell model (MCSM)

Basic idea of MCSM

- Can a complicated nuclear many-body state be approximated by a small number of “basis” states?

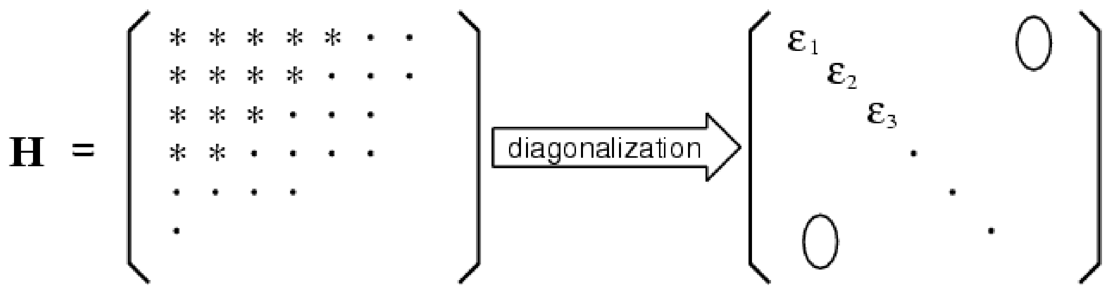

Conventional Shell Model
all Slater determinants

Monte Carlo Shell Model
bases important for a specific eigenstate

T. Otsuka, M. Honma, T. Mizusaki, N. Shimizu and Y. Utsuno, Prog. Part. Nucl. Phys. 47, 319 (2001).

Brief history

- Quantum Monte Carlo Diagonalization method (1995)
  - tested with the IBM model
- Reformulation for the shell model (MCSM) (1996)
- Several improvements and applications (until ~2005)
  - Implementing variational procedure
  - Implementing quantum number projection
  - Implementing Lawson's prescription
  - Application to full pf shell, sd-f7/2-p3/2 shell, …

this talk

- New generation of MCSM (since 2009)
  - Energy variance extrapolation method
  - Efficient computation (algorithm, coding, …)
  - Application to ab initio shell model, large systems with core

Abe's talk

Background of MCSM

- Basis states: follow auxiliary field Monte Carlo approach (the shell model Monte Carlo (SMMC) by Koonin et al.)
- exp(-βH): projector onto the ground state when β→∞
  - exp(-βH)|Ψ>: cannot be obtained for a two-body operator H
  - Hubbard-Stratonovich transformation

    for $\hat{H} = \varepsilon\hat{\mathcal{O}} + \frac{1}{2}V\hat{\mathcal{O}}\hat{\mathcal{O}}$

    $$e^{-\beta\hat{H}} = \sqrt{\frac{\beta\,|\,V\,|}{2\pi}}\int_{-\infty}^{\infty} d\sigma e^{-(1/2)\beta|V|\sigma^2} e^{-\beta\hat{h}}\,; \qquad \hat{h} = \varepsilon\hat{\mathcal{O}} + sV\sigma\hat{\mathcal{O}}$$

    σ: auxiliary field
  - exp(-βh)|Ψ>: Slater determinant when |Ψ> is a Slater determinant. However, integration over σ is needed.
- In SMMC, Monte Carlo integration is carried out.

Original MCSM procedure

- In MCSM, Monte Carlo integration is not carried out. Instead, σ's are regarded as generators of basis states.

$$|\Phi(\sigma)\rangle \propto e^{-\beta h(\sigma)} |\Psi^{(0)}\rangle$$

- Many-body states are made from $|\Phi(\sigma_1)\rangle$, $|\Phi(\sigma_2)\rangle$, … by diagonalizing the Hamiltonian in a space spanned by those basis states.

Implementing variational procedure

- A series of $|\Phi(\sigma_1)\rangle$, $|\Phi(\sigma_2)\rangle$, … contains useless basis states which barely contribute to improving the energy.
- Search for efficient basis states: trial and error
  Consider $|\Phi(\sigma_1)\rangle$, $|\Phi(\sigma_2)\rangle$, …, $|\Phi(\sigma_n)\rangle$ are already fixed and a good $|\Phi(\sigma_{n+1})\rangle$ is sought.
  1. Candidate for $|\Phi(\sigma_{n+1})\rangle$ is generated, and the energy is obtained with $|\Phi(\sigma_1)\rangle$, …, $|\Phi(\sigma_{n+1})\rangle$.
  2. Shift σ_{n+1} slightly and calculate energy. If energy becomes lower, this σ replaces σ_{n+1}. If not, try another σ.
  3. This is repeated until good convergence is attained.

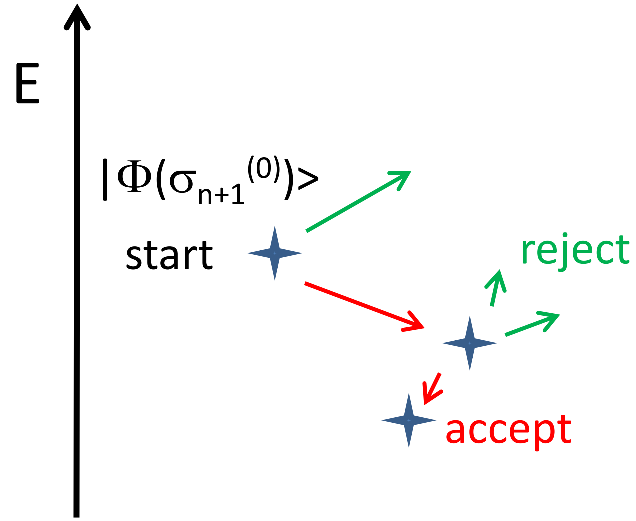

Implementing symmetry restoration

- Since each $|\Phi(\sigma)\rangle$ is a general Slater determinant, it does not have good quantum numbers that the Hamiltonian possesses (such as total angular momentum).
- In estimating the energy, $P|\Phi(\sigma)\rangle$ is considered instead of $|\Phi(\sigma)\rangle$, where P is the projector onto a desired quantum number (J=0, 2, …, etc.)
- To summarize, the MCSM wave function is expressed as

$$\left|\Psi_{JM}\right\rangle = \underbrace{\sum_{k=1}^{N_{MCSM}} c^{(k)}}_{\text{superposition}} \underbrace{P^{\pi} \sum_{K=-J}^{J} g_K{}^{(k)} P^J_{MK}}_{\text{projection}} \underbrace{\left|\Phi(D^{(k)})\right\rangle}_{\text{basis state}}$$

$$\left|\Phi(D)\right\rangle = \prod_k a(D)_k^+ \left|-\right\rangle \quad a_k^+ = \sum_i D_{ik} c_i^+$$

Effective use of parallel computers

- Angular momentum projection
  - Three dimensional integration (~10^4 mesh points) can be done independently.
- Introducing a workstation-based cluster for exclusive use of MCSM named Alphleet (in 1999).

- consists of 140 CPUs (cores)
- highest top500 rank: 169.
- Effective performance: 61.3 GFLOPS
- cost: ~ a million dollars

Alphleet Cluster

Site:	Institute of Physical and Chemical Res. (RIKEN)
System URL:	
Manufacturer:	Hewlett-Packard (Compaq)
Cores:	140
Power:	
Memory:	
Interconnect:	Myrinet
Operating System:	N/A

Configurations

List	Rank	System	Vendor	Total Cores	Rmax (GFlops)	Rpeak (GFlops)	Power (kW)
11/2000	435	Alphleet Cluster	Hewlett-Packard (Compaq)	140	61.30	140.00	
06/2000	232	Alphleet Cluster	Hewlett-Packard (Compaq)	140	61.30	140.00	
11/1999	169	Alphleet Cluster	Hewlett-Packard (Compaq)	140	61.30	140.00	

Demonstration of efficiency

- ^{56}Ni in the full pf shell
  - 10^9 m-scheme dimension: Several groups competed about a decade ago for obtaining the energy as low as possible.

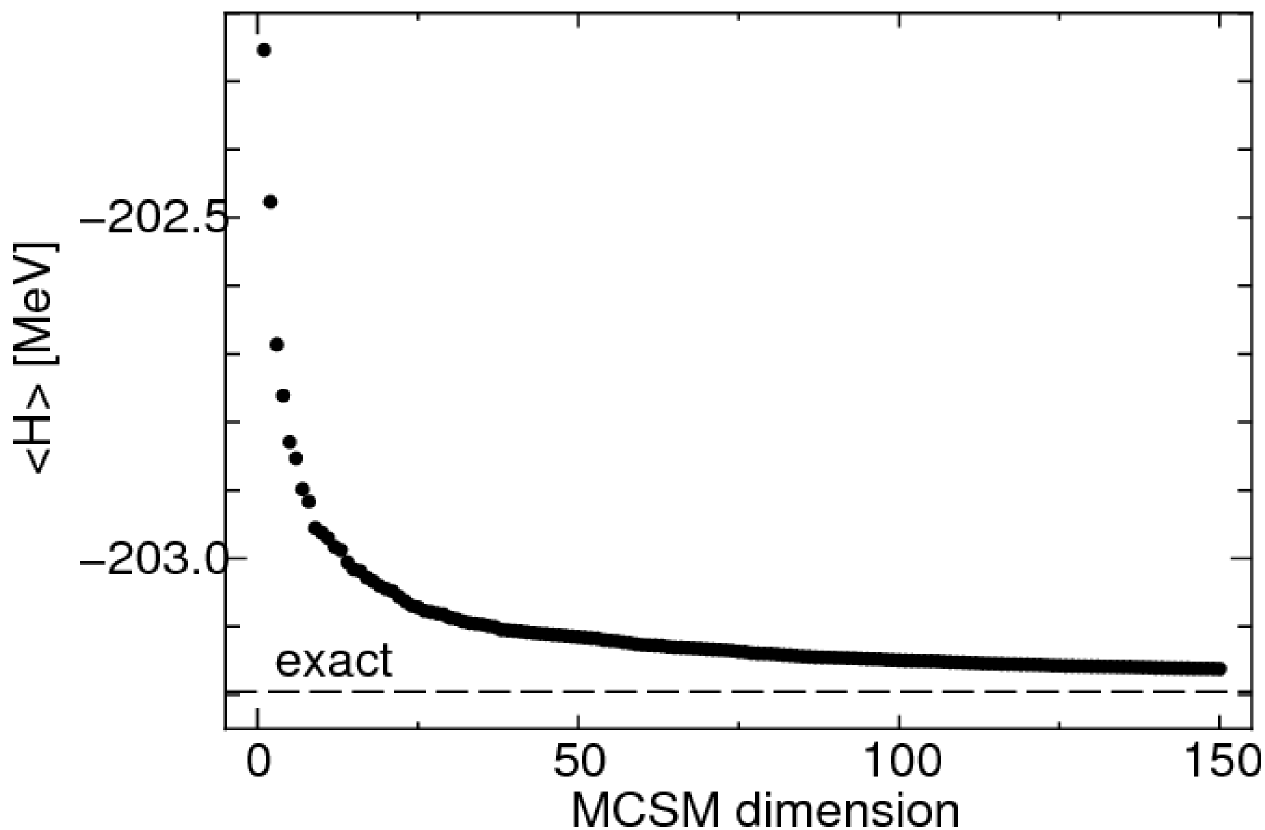

Exact: obtained after the MCSM calc.

The g.s. energy can be precisely estimated with extrapolation. (Abe's talk).

Comparison with other calculations

- M-scheme basis dimension: ~10^9
  - It was not feasible to perform the exact calculation until ~2004.

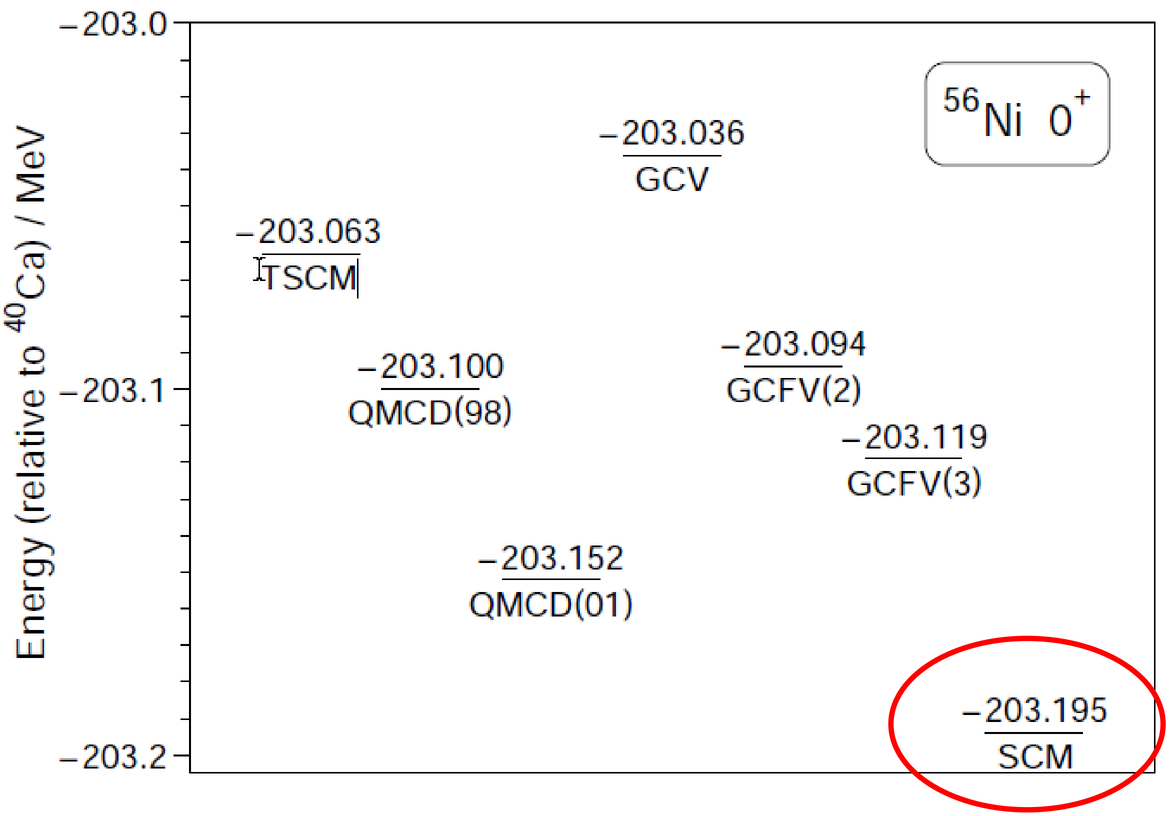

QMCD: MCSM
GCFV: VAMPIR calc.
TSCM: 6p-6h truncation
SCM: exact

Taken from K.W. Schmidt, Prog. Part. Nucl. Phys. 52, 565 (2004).

Deformed-spherical shape coexistence

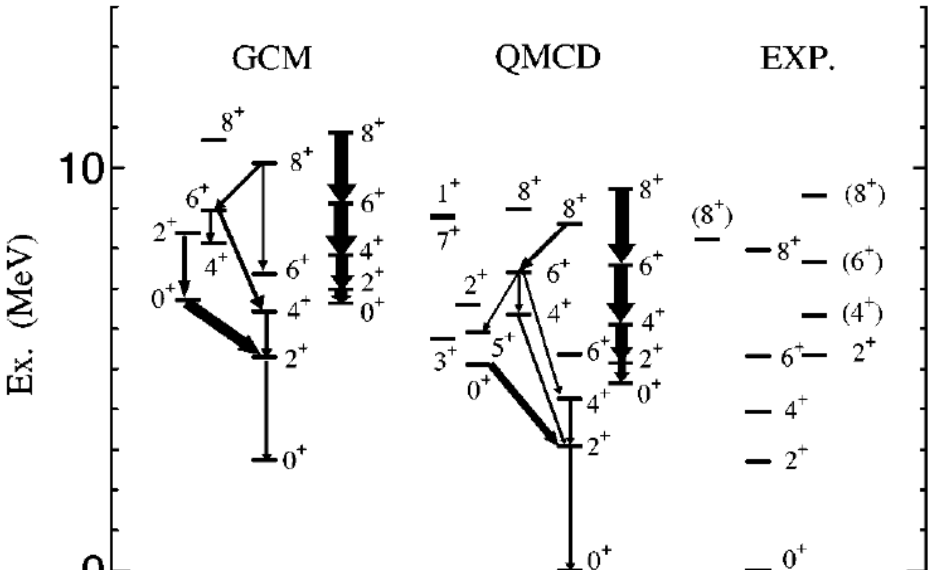

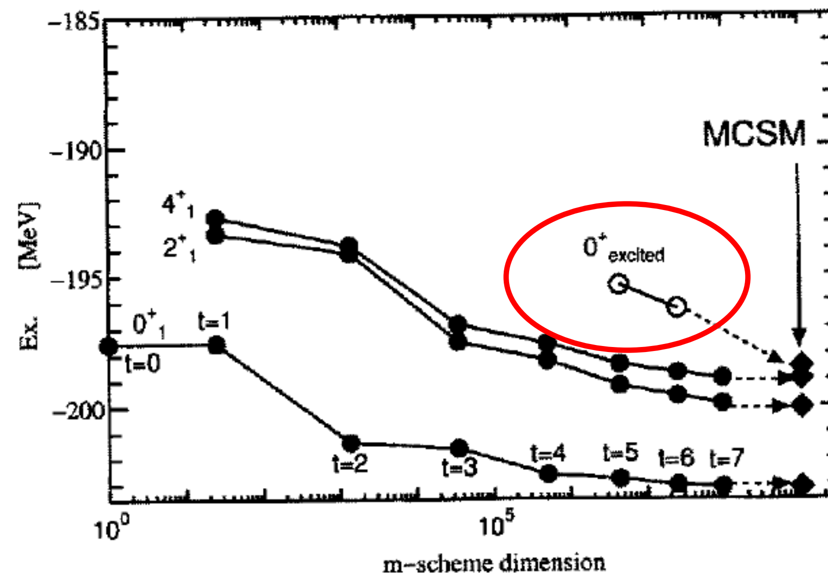

- The usual truncation (restricting the number of nucleons in sub shells) is not good for strongly deformed states.

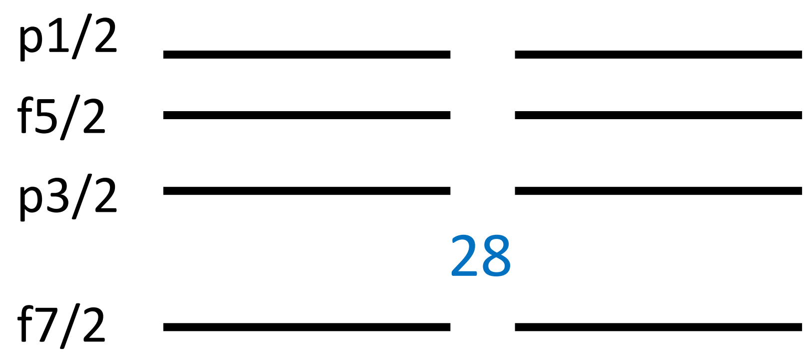

Structure of exotic nuclei around N=20

Disappearance of the N=20 magic number

Mg isotopes

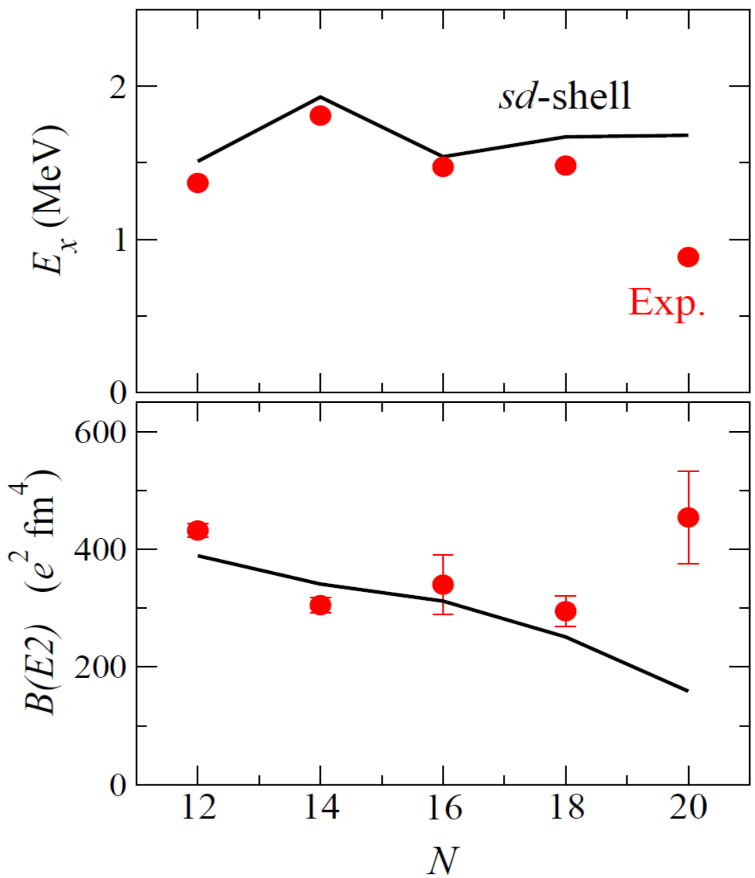

Ref.) D.Guillemaud-Mueller *et al.*, NP**A426**, 37 (1984).
T. Motobayashi *et al.*, PLB **346**, 9 (1995).

normal state (0p0h)

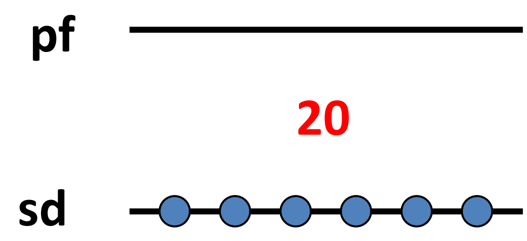

vs.

intruder state (2p2h)

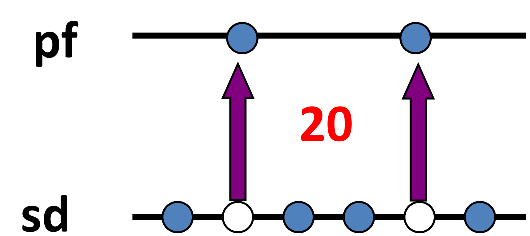

Viewpoint of the deformed shell model

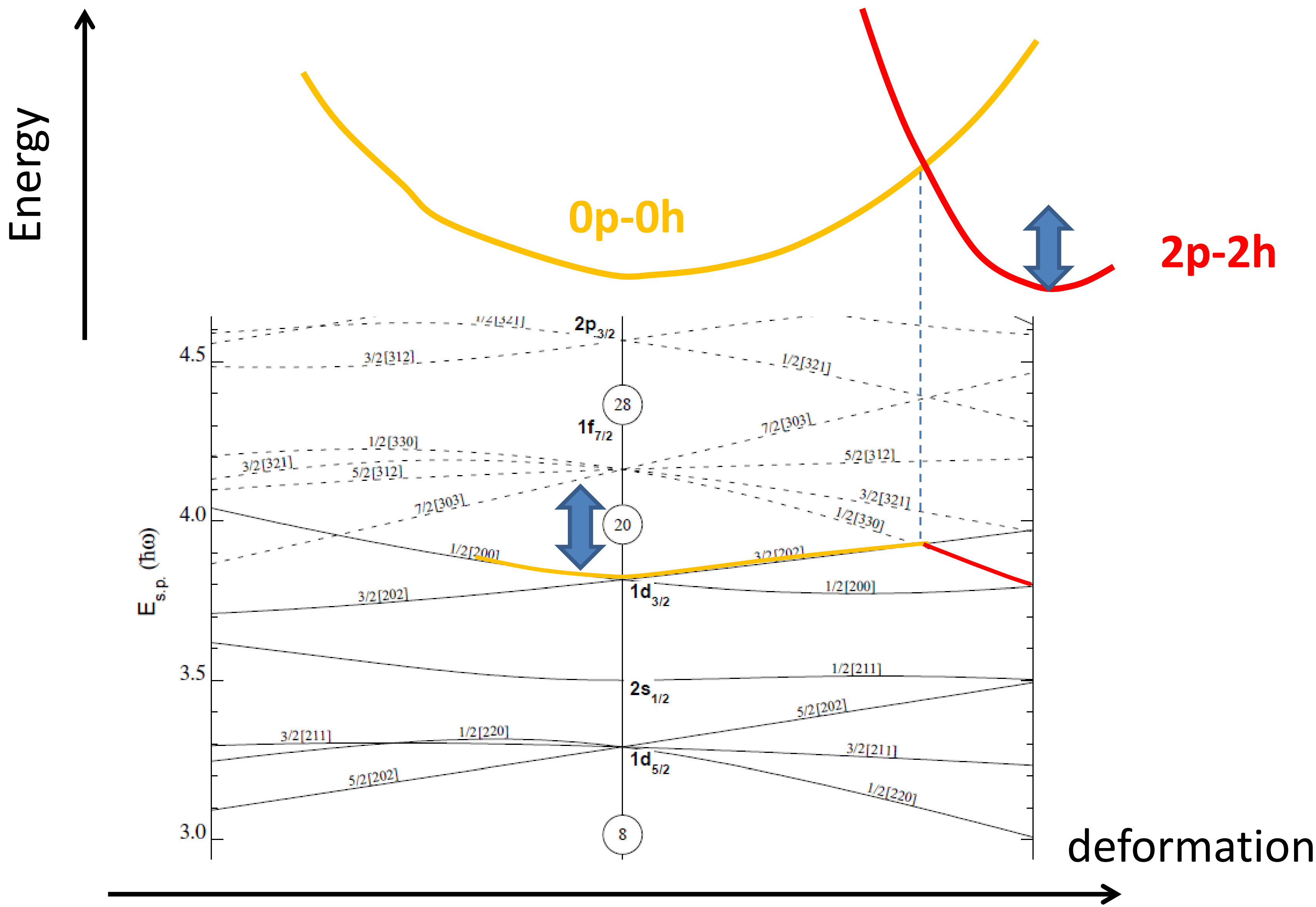

Island of inversion

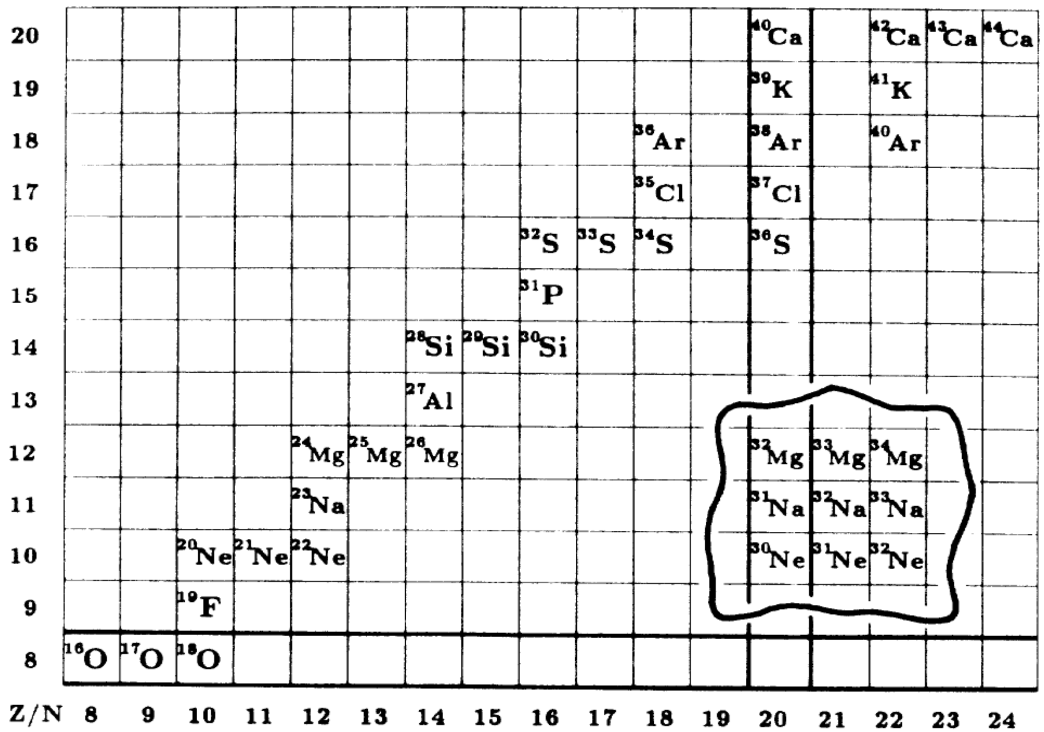

E.K. Warburton et al., Phys. Rev. C 41, 1147 (1990).

- Nine nuclei dominated by 2p-2h: prediction from (approximated) shell-model calculation

Drip line of oxygen and fluorine: another unexpected property

- Oxygen (Z=8)
  - The last bound isotopes is located at N=16 with a considerably large separation energy.
- Fluorine (Z=9)
  - The isotope with N=22 is known to be a bound nucleus. The separation energy should be kept small from N=18.

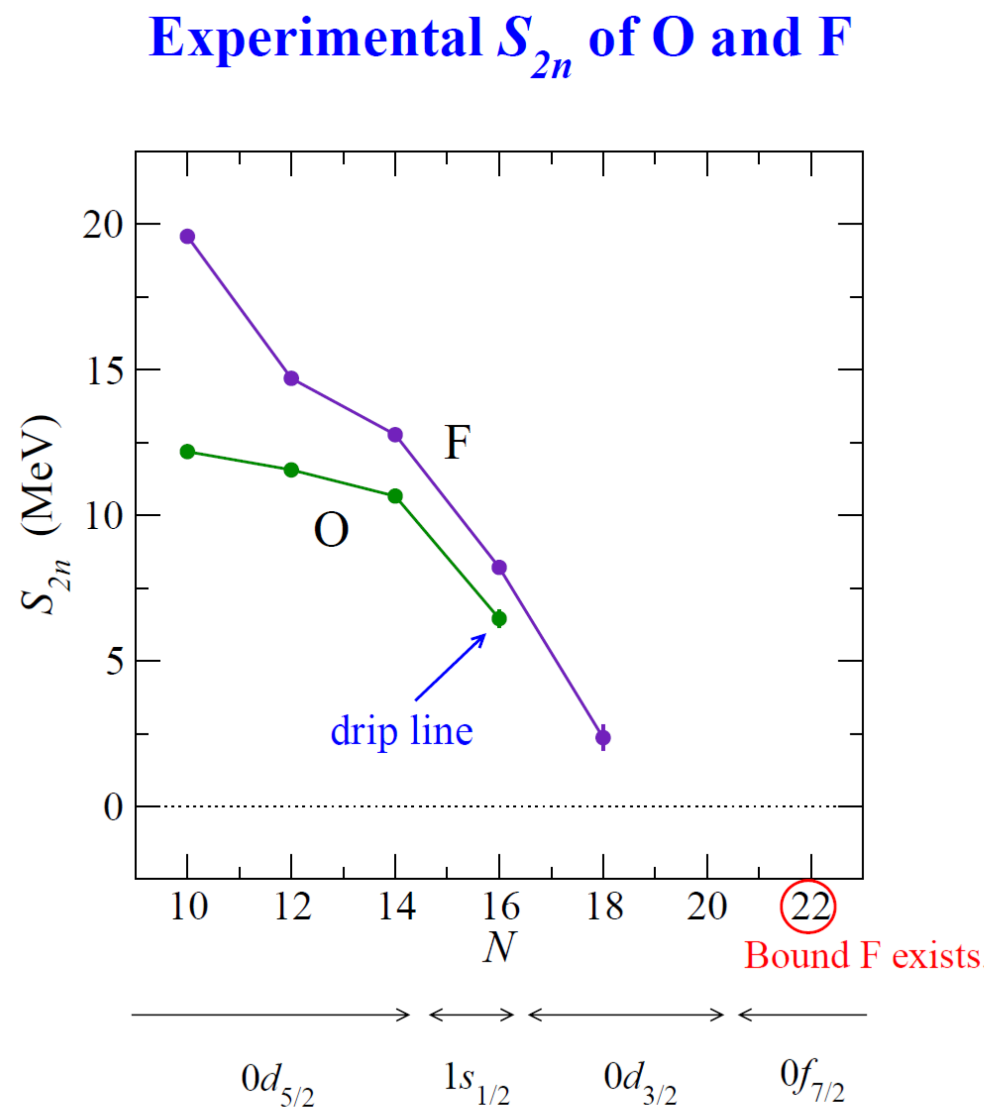

Phenomenological explanation

i) Normal shell structure

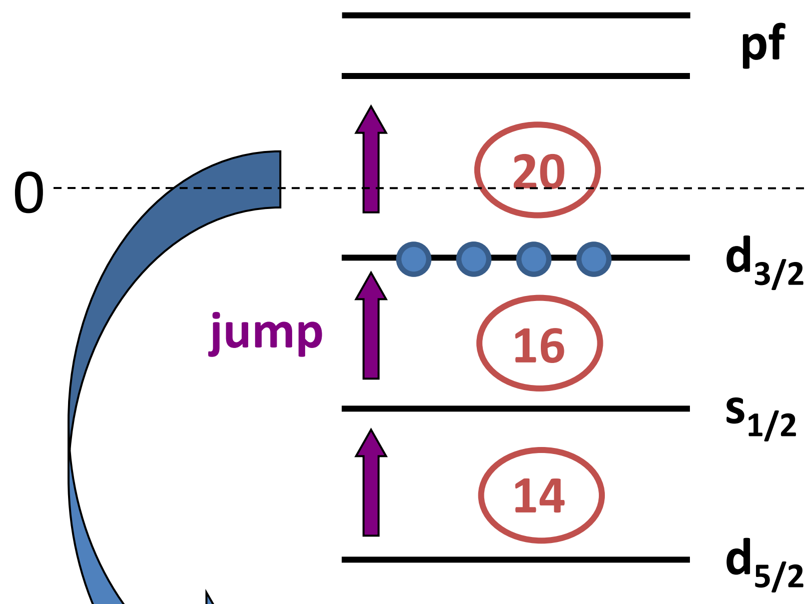

If there is a certain N=20 shell gap in F, the drip line would not persist so far away (at most 4 in $d_{3/2}$).

ii) Quenched N=20 shell gap

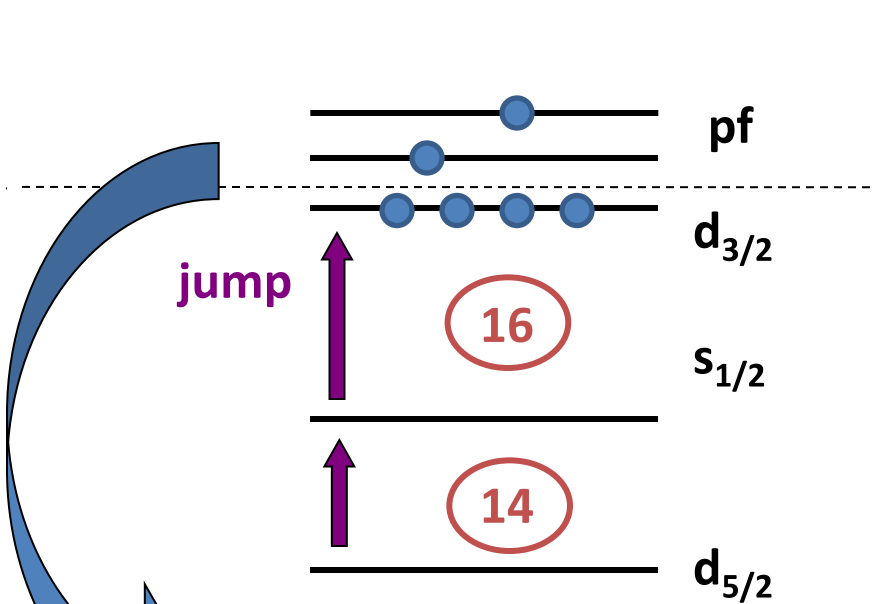

Large correlation energy due to the degeneracy can extend the drip line further.

What is obtained with the shell model

- An anomalous shell structure is expected, but observed states are not pure single particle states. A description with appropriate treatment of correlation is needed.
  → shell model calculation
- Nevertheless, the observed state is strongly affected by the shell structure. It is desirable to pin down the evolution of the shell structure and to provide its mechanism.
  → effective single-particle energy

Effective single particle energy

- Effective single-particle energy (ESPE):
  Shell-model viewpoint of generalized SPE
  - Filling configuration is assumed for the A-nucleon system.
  - Additional binding energy in the (A+1) nucleon system defines ESPE.
  - Total energy for a fully occupied system can be evaluated simply by counting the number of “bonds” and their **monopole** centroids.

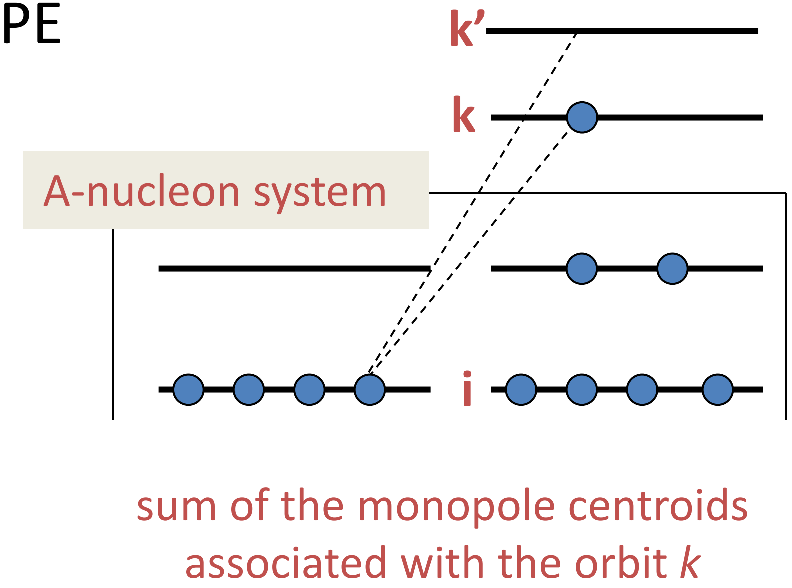

$$V_{i,j}^{T} = \frac{\sum_J (2J+1)\langle i, j|V|i, j\rangle_{J,T}}{\sum_J (2J+1)}$$

  - Orbital dependence of the monopole centroid causes the **shell evolution**.
    ($V_{i,k} \neq V_{i,k'}$ gives rise to the variation of the shell gap.)

Proposed shell structure changing from oxygen to calcium

- Neutron $d_{3/2}$: main player
  - stays high around oxygen: N=16 magic number
  - comes down around calcium: (normal) N=20 magic number
  - contributes to the inversion
- Strongly attractive $d_{5/2}$-$d_{3/2}$ interaction

Neutron ESPE

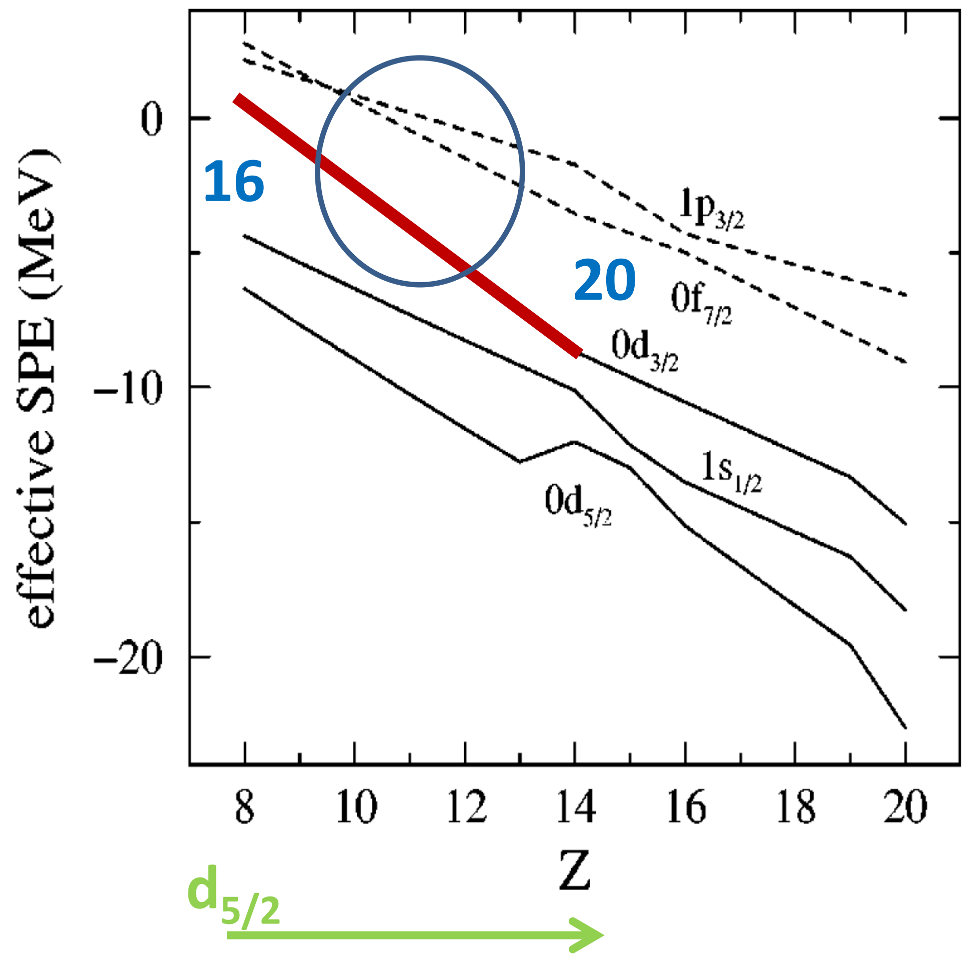

How do we make an effective interaction with that single-particle structure

- Model space: full sd shell + $f_{7/2}$ + $p_{3/2}$
- Starting point: existing effective interactions
  - USD (Wildenthal and Brown): sd shell part
  - Kuo-Brown: pf shell part
  - Millener-Kurath: cross shell part
- Modification of the monopole interaction

$$\delta V^{T=1,0}_{0d_{5/2},0d_{3/2}} = +0.30, -0.70\,\mathrm{MeV},$$

$$\delta V^{T=1,0}_{0d_{5/2},0f_{7/2}} = +0.16, -0.50\,\mathrm{MeV},$$

} named SDPF-M

↓

shell structure shown in the last slide

minimal change for this aim

Overview of the yrast properties

Energy levels

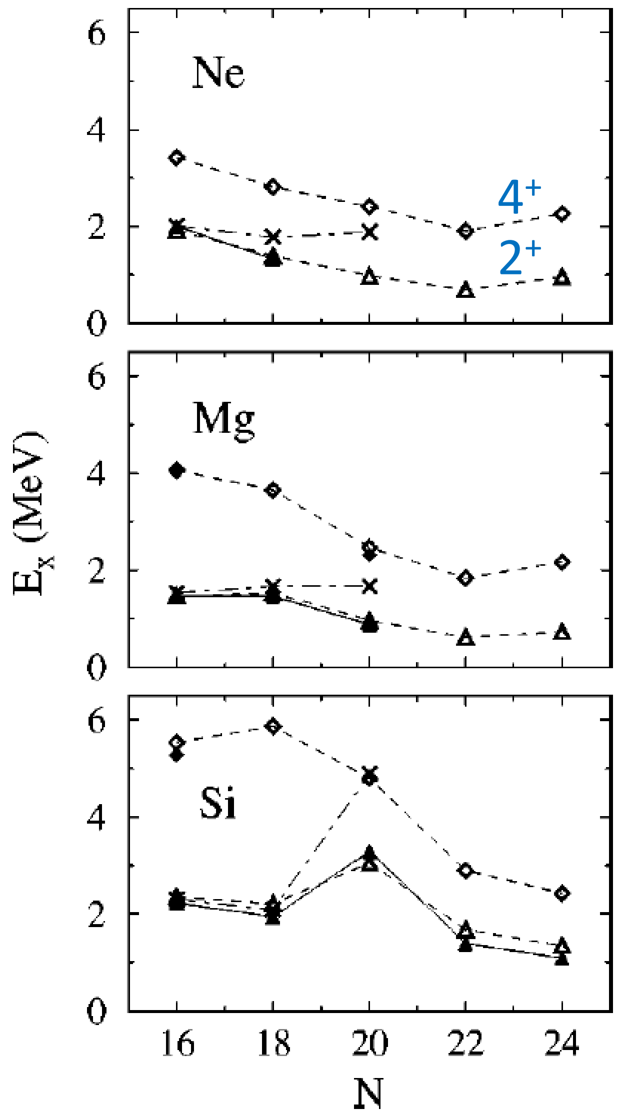

B(E2) values

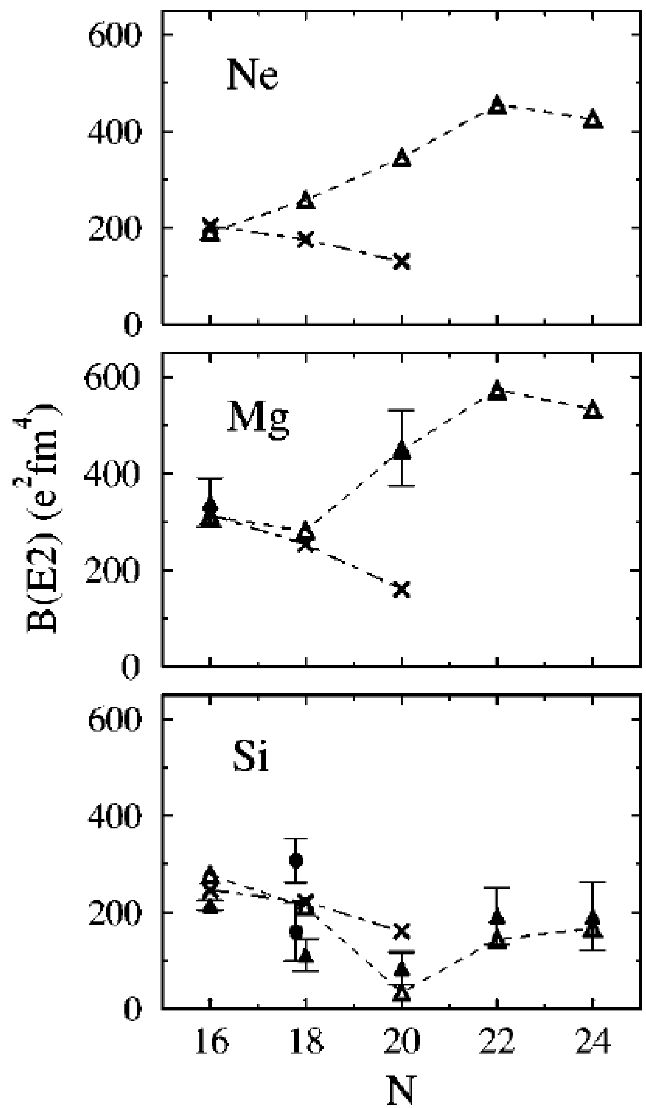

Importance of determining “western” boundary

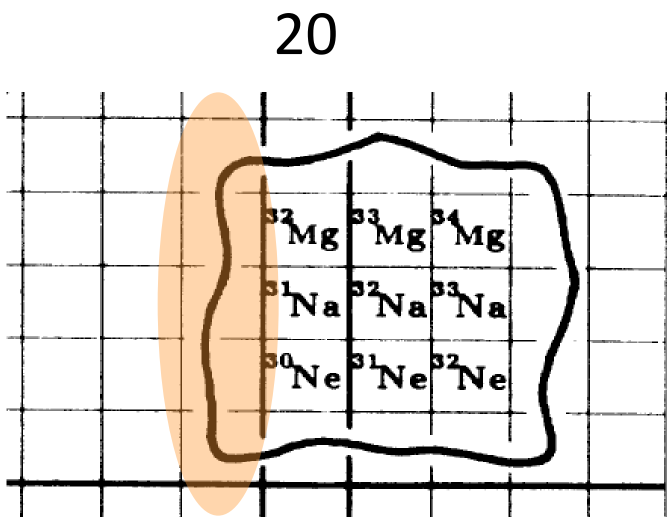

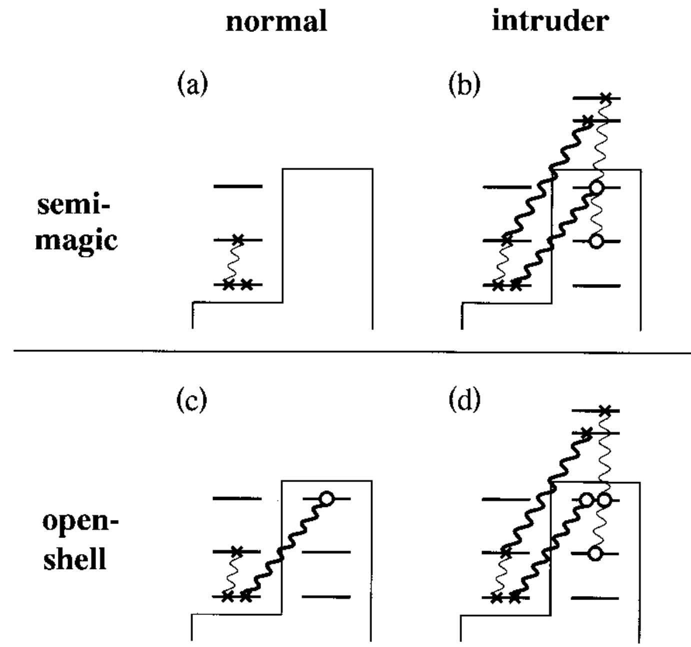

difference in corr. energy

largest

smaller

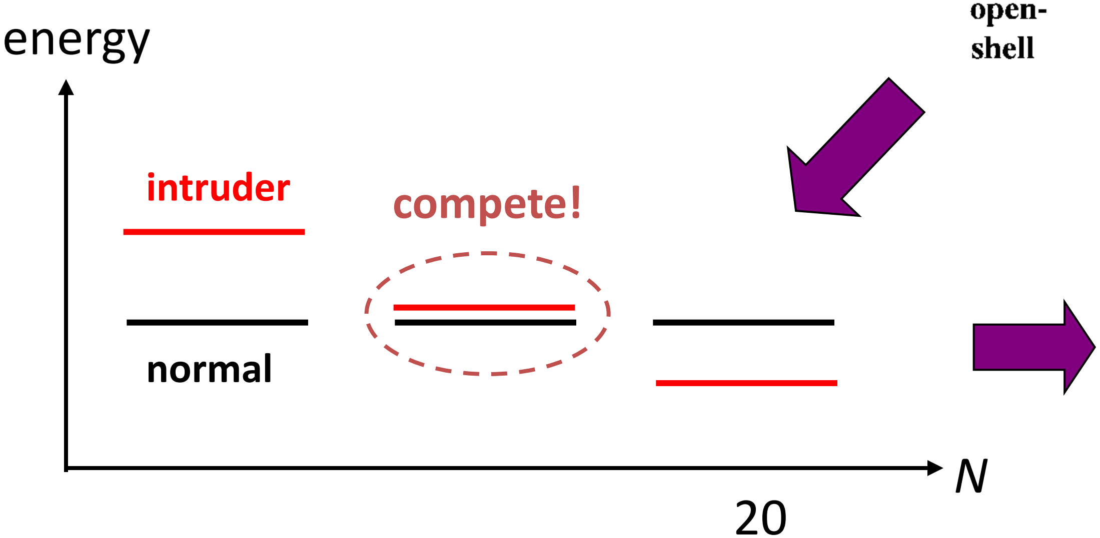

The location of the western boundary is quite sensitive to the shell gap.

Case of Na (Z=11) isotopes

- Electromagnetic moment
  - good probe for the wave function
- Comparison between theory and experiment
  - The N=19 isotope is clearly inside the island of inversion contrary to the original mapping.
- larger island with indistinct boundary due to the narrow N=20 shell gap

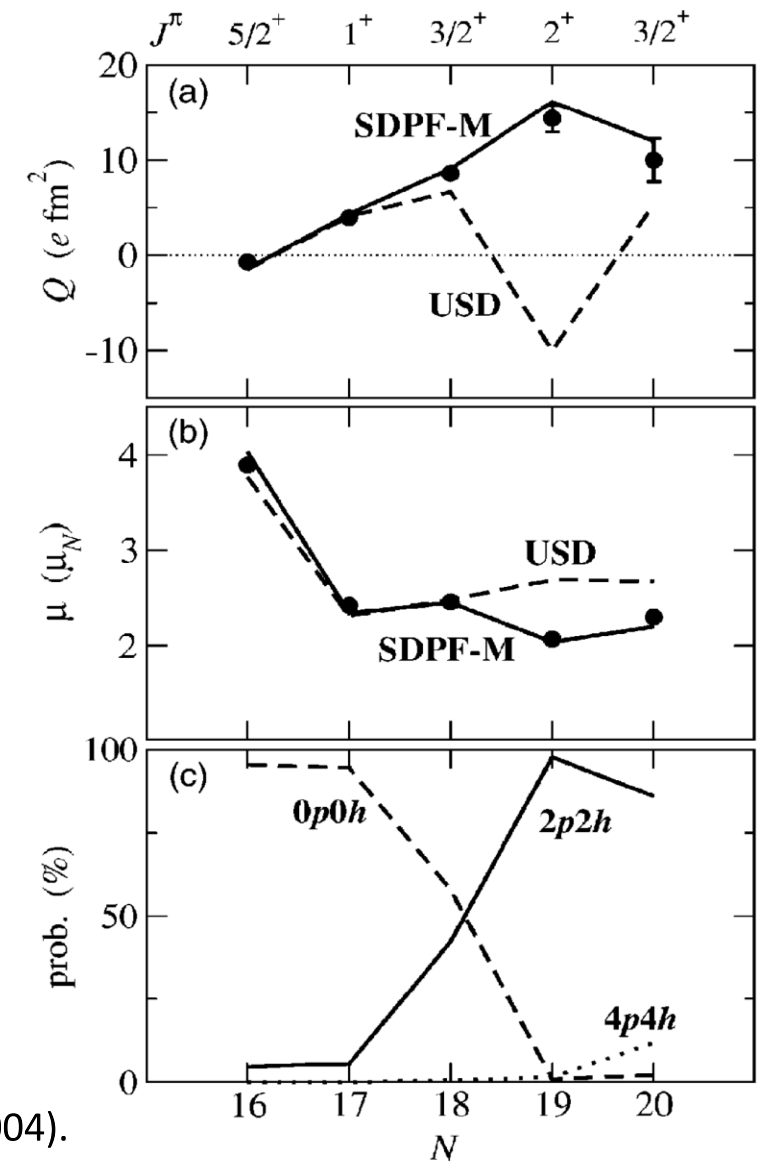

Y. Utsuno et al., Phys. Rev. C 70, 044307 (2004).

Recent understanding of the shell evolution

Origin of the difference in monopole interaction

- $V_{ij} \neq V_{ik}$ causes the evolution of the shell structure.
- Strong dependence on spin direction
  - Strong attraction between $j_>$ and $j_<$ (such as $d_{5/2}$ and $d_{3/2}$)
- $(\tau\cdot\tau)(\sigma\cdot\sigma)V(r)$?
  - demonstrated to cause a plausible effect at the long range limit
  - However, the spin dependence is too small in realistic systems.
- Another origin?

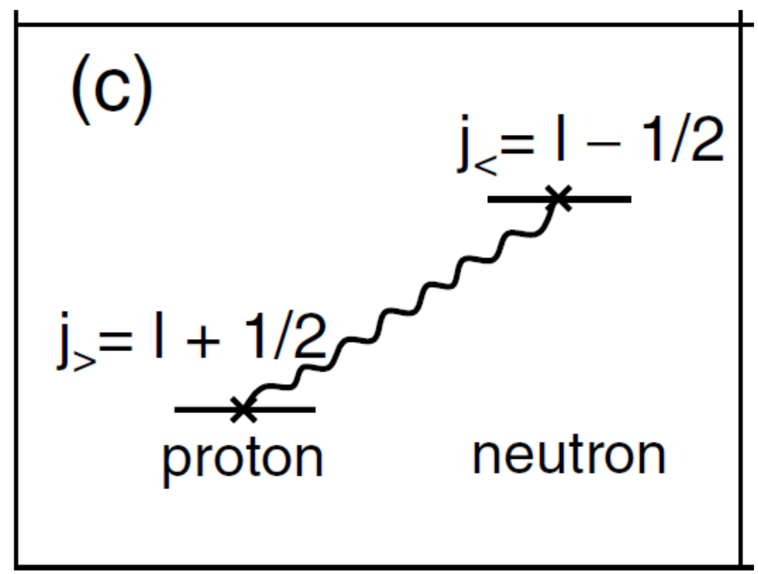

T. Otsuka et al., Phys. Rev. Lett. 87, 082502 (2001).

Tensor force

- Regarded as an important part as the bare force, but often omitted as the effective interaction (Skyrme, Gogny, …)
  - dominance of the second-order effect (e.g., no effect on the spin-saturated mean-field wave functions such as ^{16}O)
- Revival of the tensor force as the effective interaction
  - Not large effect on the total energy, but large contribution to the shell energy
  - Evolution of the ls splitting due to

$$(2j_> + 1)V^T_{j_>,j'} + (2j_< + 1)V^T_{j_<,j'} = 0,$$

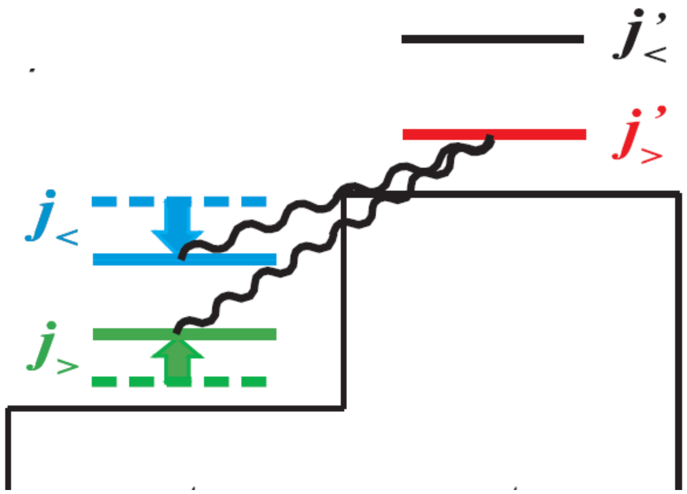

T. Otsuka et al., Phys. Rev. Lett. 95, 232502 (2005).

Evolution of energy levels in antimony isotopes

- Sb (Z=51): dominance of proton single-particle level
  - supported by proton transfer experiment
    (J.P. Schiffer et al., Phys. Rev. Lett. 92, 162501 (2004).)
  - The tensor force (included in GT2) reproduces experiment.

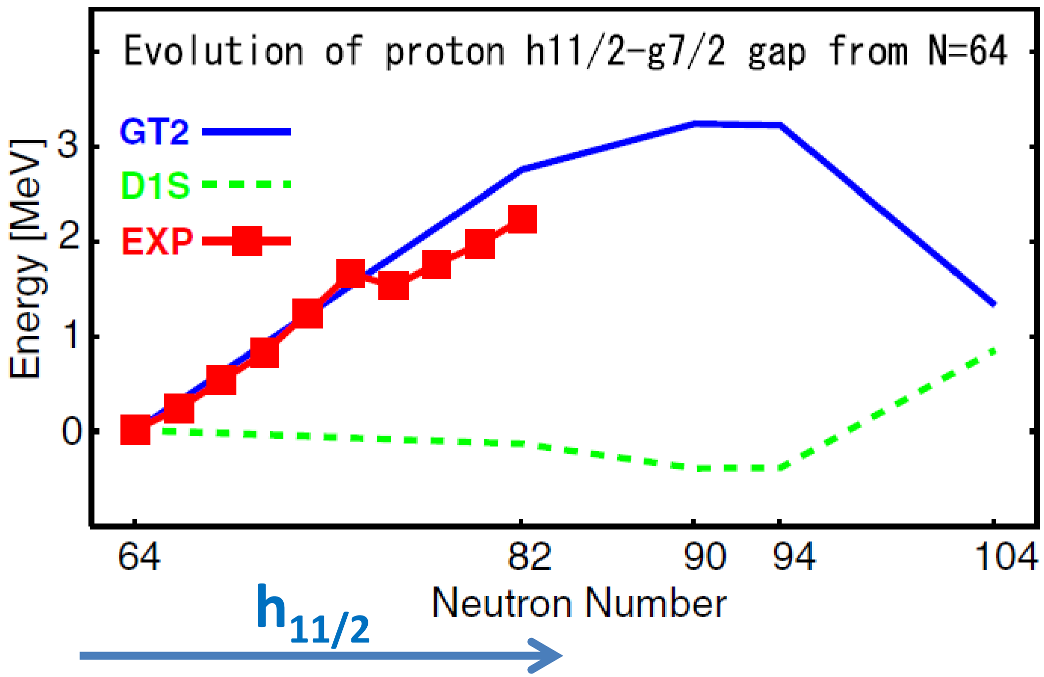

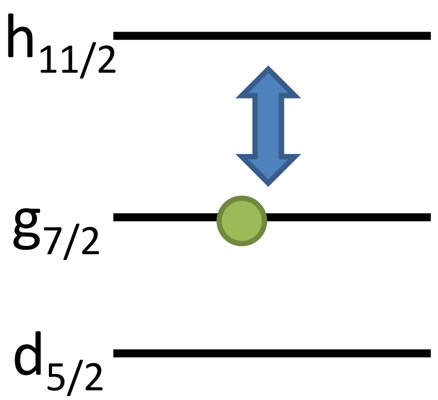

Persistency of the tensor force

- How strong is the tensor force as the effective interaction?
  - Model space dependence?
- Analysis by a microscopic effective interaction theory
  - $V_{low\,k}$: short range correlation is treated
  - Q_{box}: in-medium effect is included further.
- Very similar to the bare (long range) tensor force

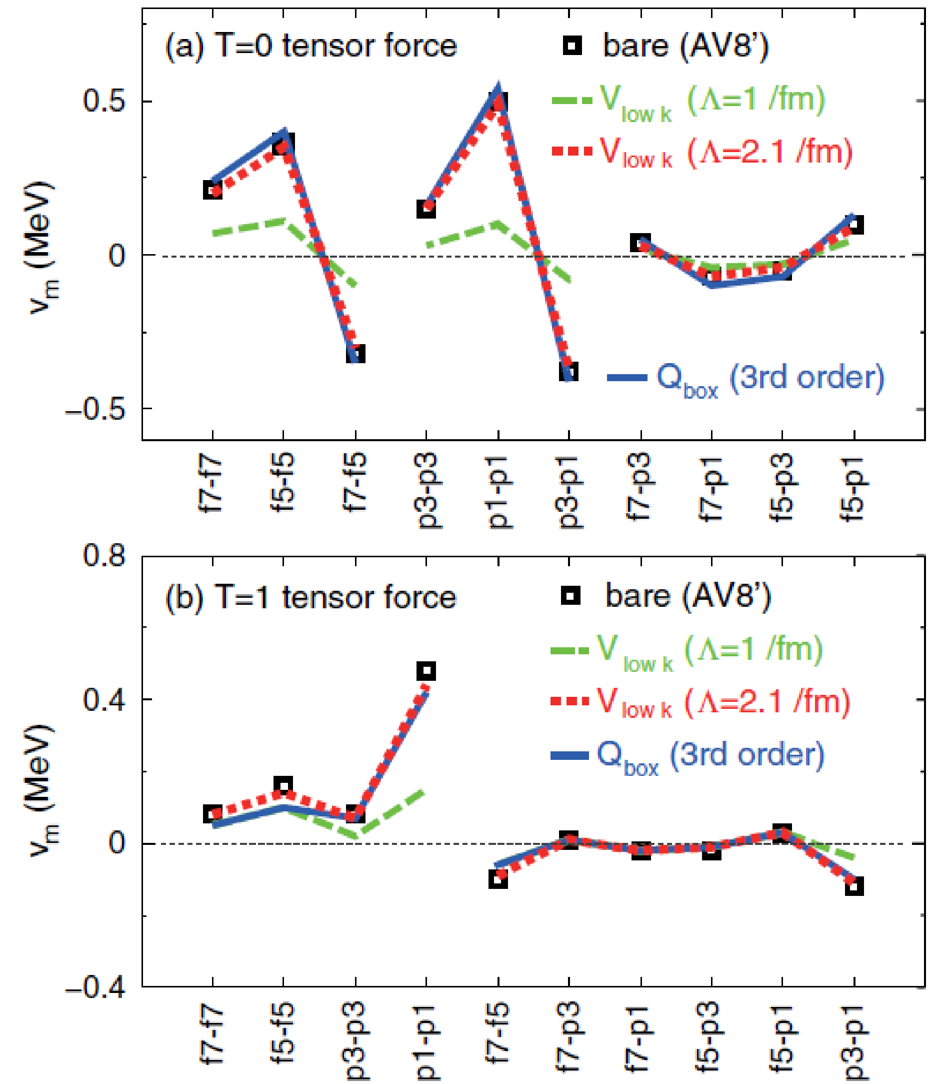

T. Otsuka et al., Phys. Rev. Lett. 104, 012501 (2010).

Comparison with empirical interaction

- GXPF1: an empirically fitted interaction for the pf shell
- The tensor part is extracted with the spin-tensor decomposition

$$V = \sum_{k=0}^{2} V_k = \sum_{k=0}^{2} U^{(k)} \cdot X^{(k)}$$

$$\langle ABLSJ'T | V_k | CDL'S'J'T \rangle$$
$$= (-1)^{J'} (2k+1) \begin{Bmatrix} L & S & J' \\ S' & L' & k \end{Bmatrix} \sum_{J} (-1)^{J} (2J+1) \begin{Bmatrix} L & S & J \\ S' & L' & k \end{Bmatrix}$$
$$\times \langle ABLSJT | V | CDL'S'JT \rangle$$

T=0 monopole centroid of the tensor force (MeV)

i	j	GXPF1	π+ρ
f7	**f7**	0.223	0.210
f7	**p3**	0.036	0.035
f7	**f5**	-0.335	-0.315
f7	**p1**	-0.073	-0.070
p3	**p3**	0.092	0.150
p3	**f5**	-0.048	-0.046
p3	**p1**	-0.229	-0.376
f5	**f5**	0.382	0.360
f5	**p1**	0.097	0.093
p1	**p1**	0.306	0.501

quite similar

Non tensor part of the monopole interaction

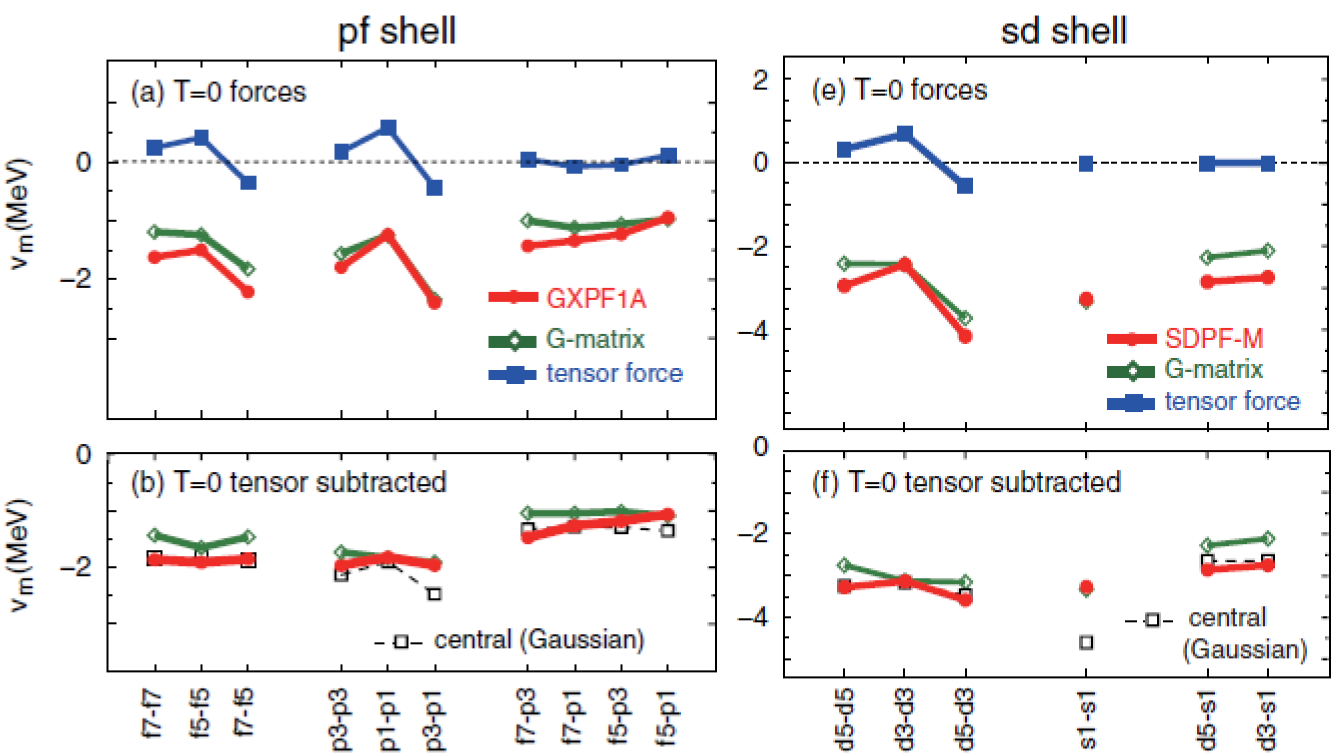

- Very mild spin dependence
- Some node dependence
- Can be fitted by a Gaussian central force

Monopole-based universal interaction (V_{MU})

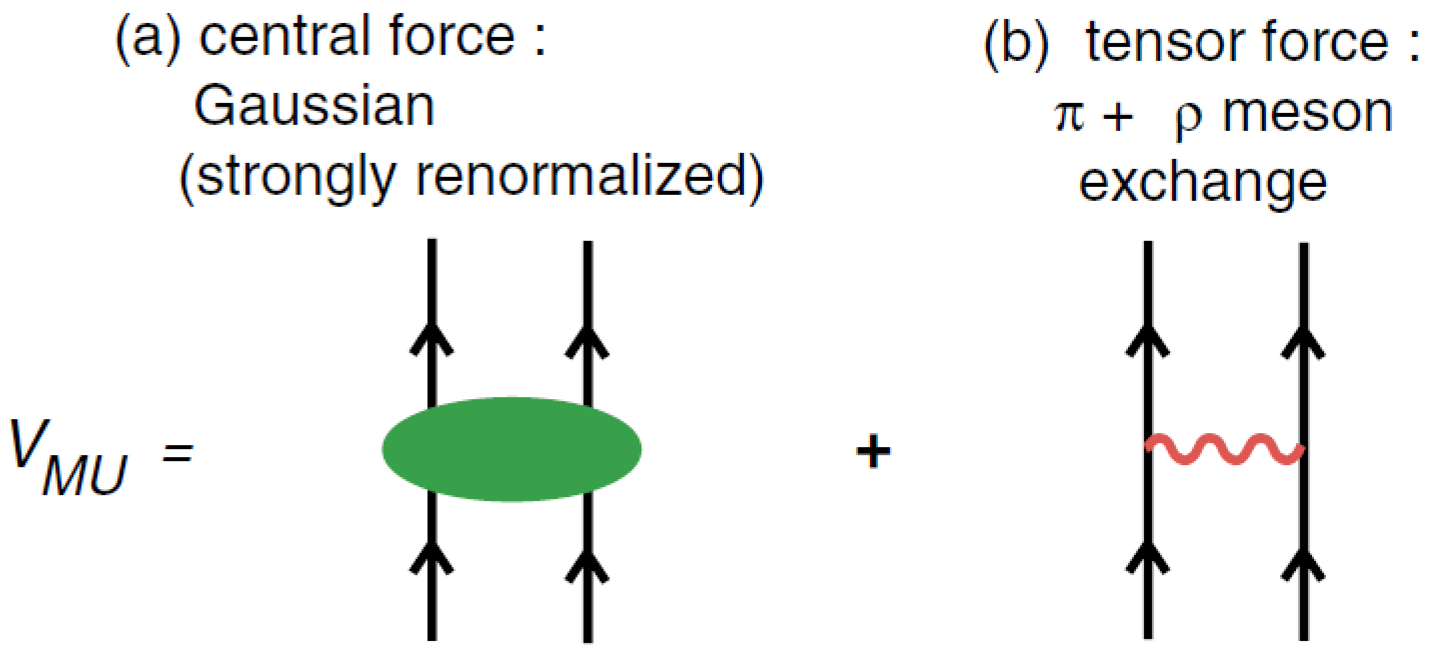

T. Otsuka et al., Phys. Rev. Lett. 104, 012501 (2010).

- Ansatz
  - Strongly renormalized central part is well approximated by the Gaussian force at least as far as the monopole part is concerned.

Application of V_{MU} to the N≈28 region

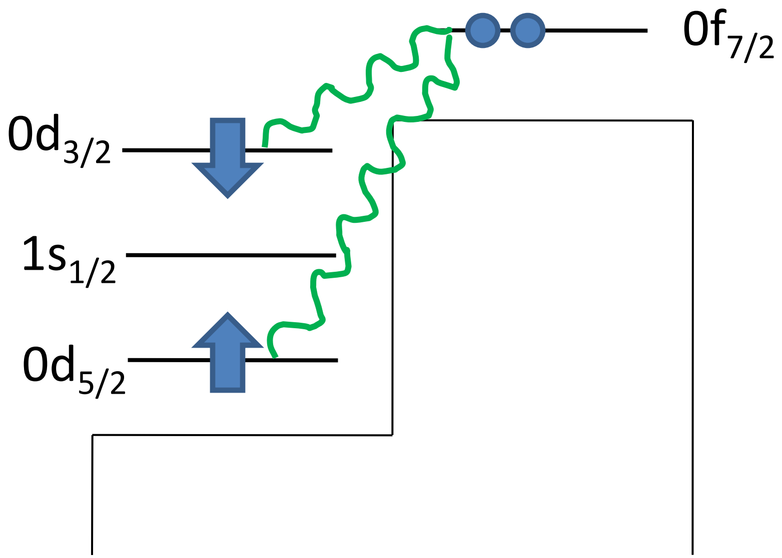

- Evolution of the sd shell from N=20 to 28 is focused.
  - cross shell part
- Effect of correlation is included by the shell model.
- Setup of the calculation
  - Full sd-pf orbit is taken, but excitation of nucleons across the N=20 is not allowed.
  - V_{MU} (slightly refined) is used as the cross shell interaction.
  - The sd shell part and the pf shell part are substituted with USD and GXPF1B (empirical interactions), respectively.

Probing the proton ls splitting

- Proton one-hole state
  - Good measure for probing the single-proton state
  - However, the $d_{5/2}$ state is strongly fragmented because of high excitation energy.
  - Distribution of the spectroscopic factor is helpful.

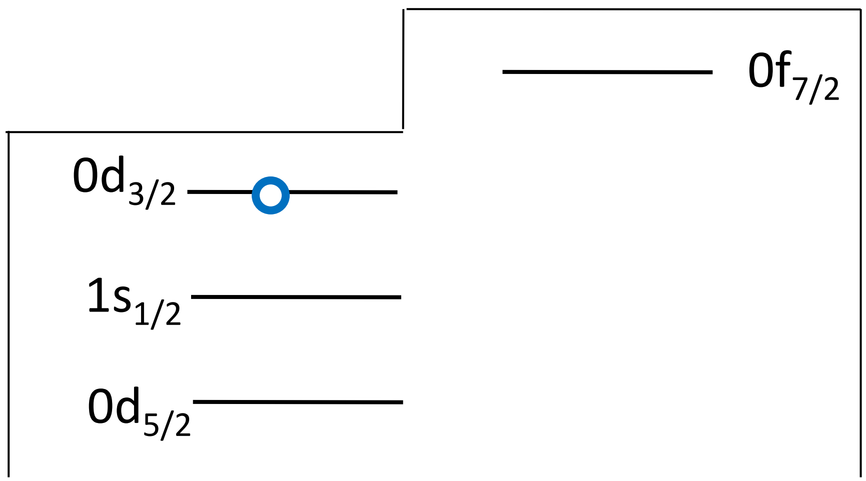

Spectroscopic factor for 1p removal from ^{48}Ca

Present interaction (w/ tensor) **w/o tensor in the cross shell int.**

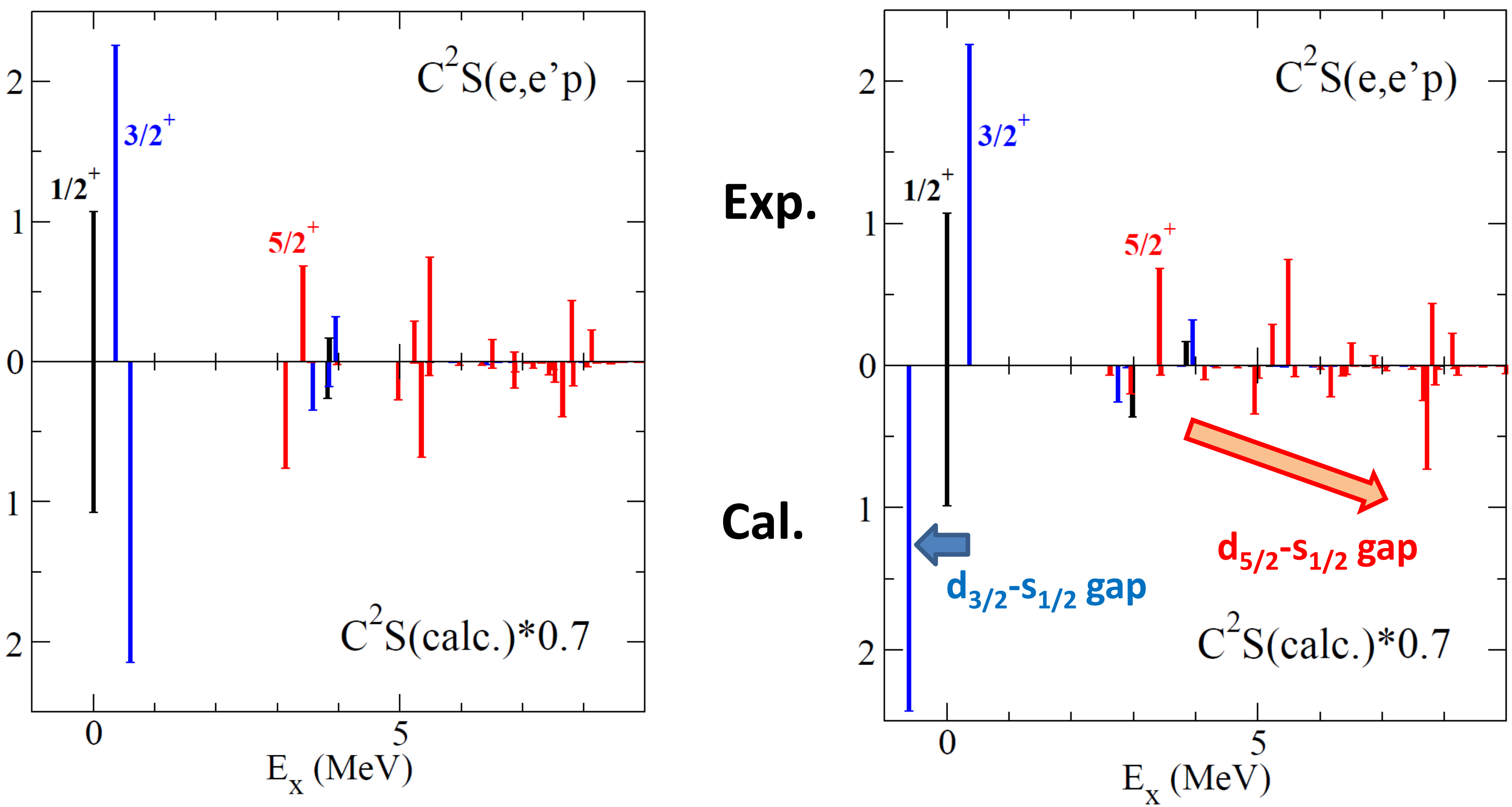

(e,e'p): G.J. Kramer et al., Nucl. Phys. A 679, 267 (2001).

Effect on collectivity: Si and S isotopes

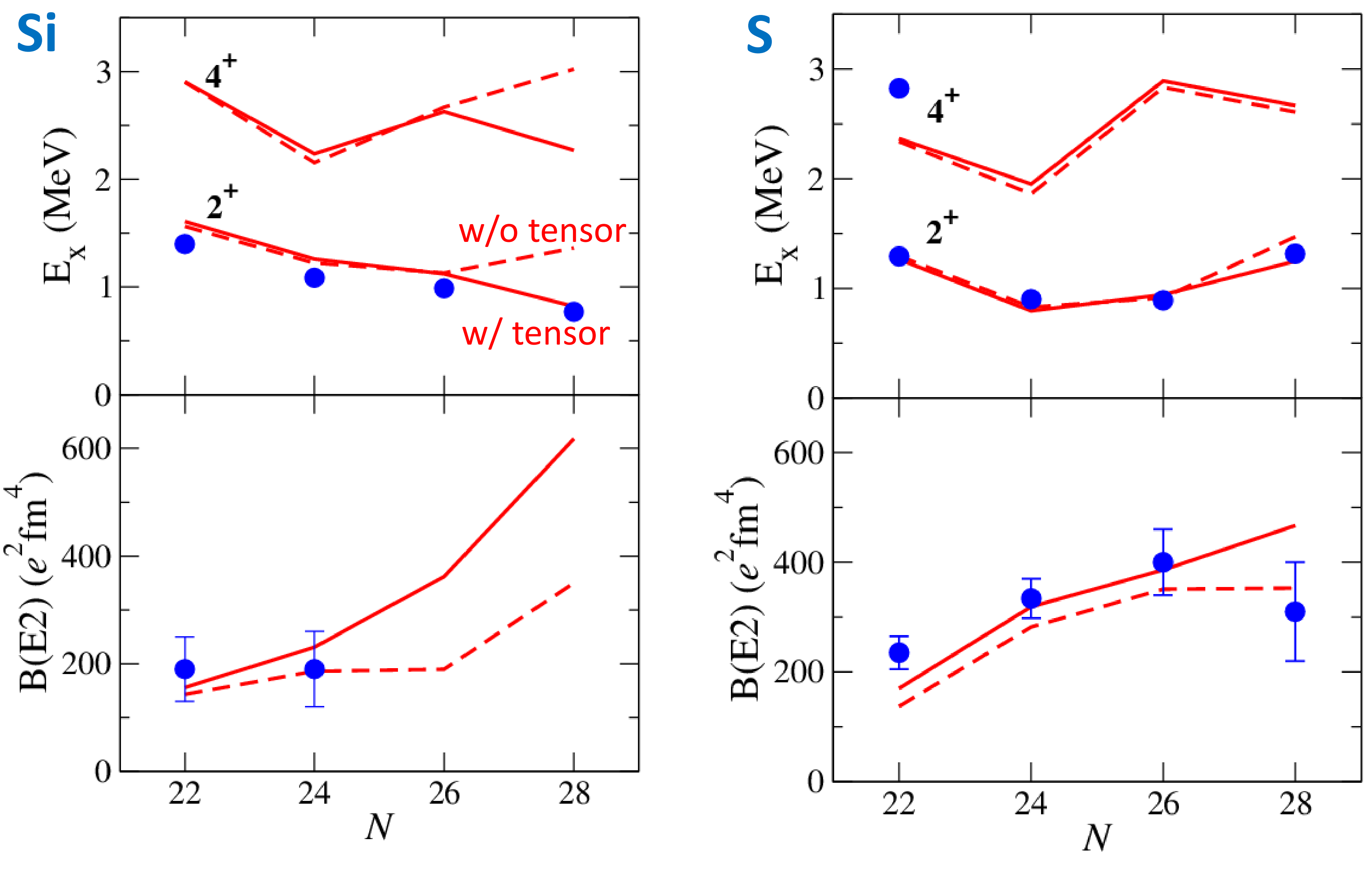

Comparison of the effective SPE

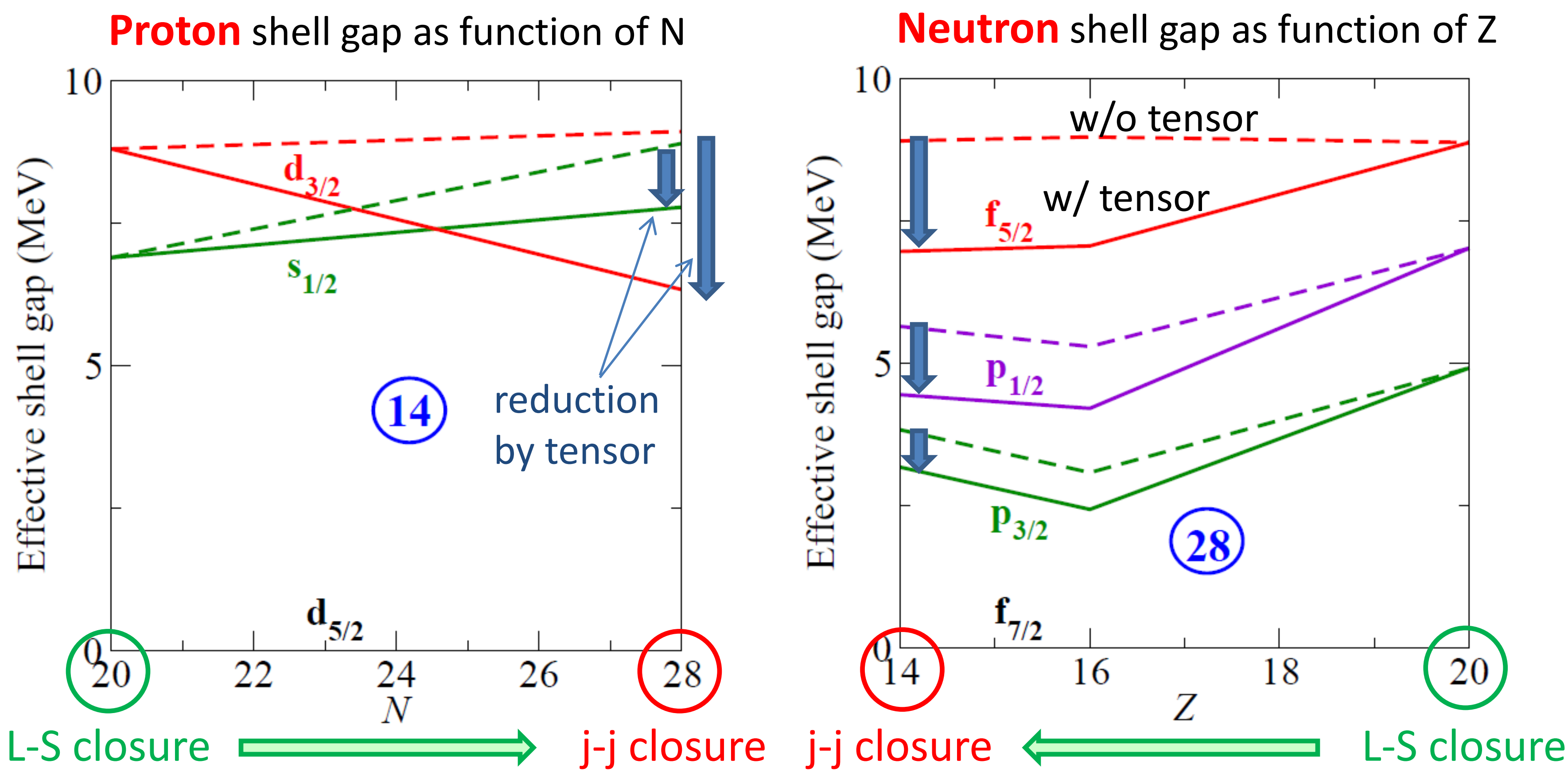

- Coherent quenching of proton and neutron shell gaps which increase toward the j-j closure

Potential energy surface

- obtained by constrained HF calc. in the shell-model space
- The tensor force drives shape to oblate deformation in Si.
  - caused by near degeneracy: Jahn-Teller effect

	^{36}Si (N=22)	^{38}Si (N=24)	^{40}Si (N=26)	^{42}Si (N=28)
with tensor				
without tensor				

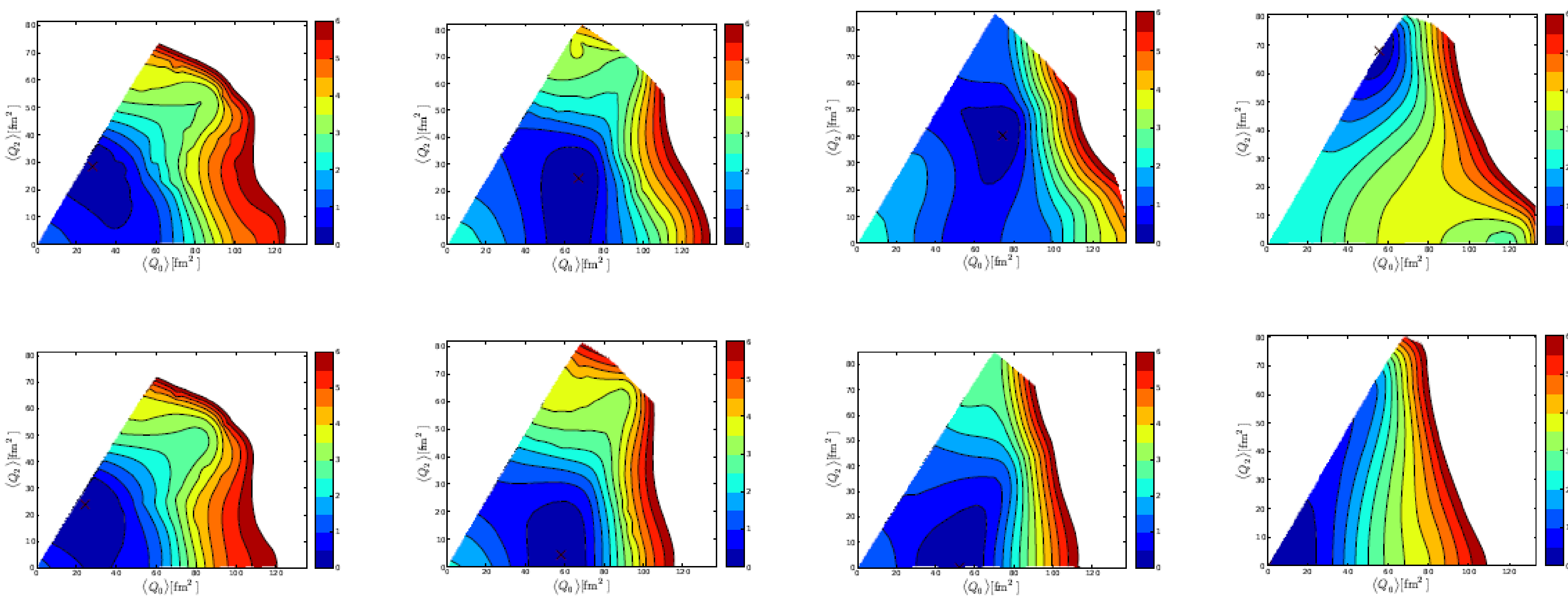

Summary

- The Monte Carlo shell model (MCSM) has been developed to overcome the limitation of conventional diagonalization.
  - Description of many-body wave function with a small number of symmetry-restored Slater determinants
- The disappearance of the N=20 magic number in neutron-rich nuclei has been studied with MCSM.
  - Correlated system; shell model calculation is helpful.
  - Effective single-particle energy, monopole interaction
- Recent understanding of the shell evolution has been shown.
  - Revival of the tensor force as the effective interaction
  - (semi-phenomenological) universal monopole interaction
  - Neutron-rich N~28 systems